Synthesis, Spectroscopic characterization, Antimicrobial, Antitumor Properties of new 4-amino-2,3 dimethyl-1-phenyl -3- pyrazolone-5-one (antipyrine) Schiff Bases and its transition metal complexes

N. G. El-Kholy

Chemistry Department, Faculty of Science (Girl' s), Al-Azhar University, Nasr City, Cairo, Egypt
nagdaelkholy2017@yahoo.com

Abstract: A Schiff base ligands L^1, L^2, L^3 were prepared from condensation reaction of 4 amino-2,3- dimethyl-1-phenyl-3-pyrazoline-5-one(4aminoantipyrine) with P. methoxybenzaldehyde (L^1), O. methoxy-benzaldehyde (L^2) and 4 hydroxy-3-methoy benzaldehyde (L^3) in absolute ethanol solution. The prepared ligands forms a series of Fe(III), Fe(II), Co(II), Ni(II), Cu(II), Zn(II), Cd(II) and Cr(III) complexes in good yield. The structures of the newly ligands and their transition metal complexes are investigated and characterized using different physicochemical studies as elemental analysis, IR spectra, ^{1}HNMR, UV-Vis spectra and solid reflectance, mass spectra, magnetic susceptibility, and thermal analysis (TGA and DTA). The spectroscopic data of the complexes suggest their 1:1 (M: L) complex structures. Also the spectroscopic studies suggest the octahydral structure for all complexes. Further, some of these complexes show lower conductance values, supporting their non electronic nature while the others complexes high conductance value supporting 1:1 electrolytic nature. Moreover the synthesized Schiff bases L^1, L^2, L^3 and their metal complexes were screened for their antimicrobial, antifungal and anticancer activity. The antimicrobial efficiency of these complexes reveals that the complex containing cobalt, cadmium and nickel exhibited the highest broad-spectrum antimicrobial activities. Also the results of antitumor activities of the purified compounds confirm that the highest inhibitory effect was reported at IC_{50} value 27.1 µg /ml for compound **(5).**
[N. G. El-Kholy. **Synthesis, Spectroscopic characterization, Antimicrobial, Antitumor Properties of new 4-amino-2, 3 dimethyl-1-phenyl -3- pyrazolone-5-one (antipyrine) Schiff Bases and its transition metal complexes.** *J Am Sci* 2017;13(2):132-145]. ISSN 1545-1003 (print); ISSN 2375-7264 (online). http://www.jofamericanscience.org. 16. doi:10.7537/marsjas130217.16.

Key word: 4 amino antipyrine, methoxybenzaldehydes, Schiff bases, transition metal complexes, antimicrobial antifungal and antitumor activity

1. Introduction

Schiff bases or azomthines with C=N in the structure are the product from the condensation reaction **[1, 2].** Schiff base ligands are considered" Privileged ligands" because they are mainly prepared by condensation between aldehyde and primary amine **[3]**. A large number of schiff base ligands have been widely applied for their interesting and important properties such as biological activities **[4,5]**, fluorescent sensor **[6,7]**, pigments and dyes, catalyst, intermediates organic synthesis and as polymer stabilizers **[8]**. The chemistry of the schiff base ligands and their metal complexes has expanded enormously and encompasses a vast area of organometallic compounds and various aspects of bioinorganic chemistry **[9]**. These ligands are able to coordinate many different metals and to stabilize them in various oxidation states **[10]**. Antipyrine and its derivatives are well known for its pharmaceutical as well as medicinal applications **[11 – 14]**. 4amino-2,3-dimethyl-1-phenyl-3-pyrazoline-5-one possesses the pyrazolone ring, which comprises of two nitrogen atoms and one ketone group. It is active moiety as a pharmaceutical ingredient, especially in the class of non sterodial anti-inflammatory agents. Prominently, these are investigated on the basis of potential biological activities such as antifungal, antibacterial, analgesic, sedative and antipretic agent **[15, 16]**. Also coordination compounds containing antipyrine derivatives have been synthesized and studied recently for their numerous applications **[17-21]**. Bio-important antipyrine derived schiff bases and their transition metal complexes were studied **[22]**.

A series of Cu(II), Co(II), Zn(II) and Ni(II) mixed ligand metal complexes were synthesized using schiff base ligand(L1) derived from condensation reaction of 4-amino-2,3-dimethyl-1-phenyl-3-pyrazoline-5-one (4amino antipyrine)with 3-phenyl-prop-2 enal (cinnamaldehyde) and knoevenagelcondensate ligand (L2) derived from penta-2,4 – dione (acetylacetone) with 3-phenyle-prop-2-enol (cinnamaldehyde in 1:1:1 molar ratio (M: L^1: L^2) **[23]**.

Following all these observations and as a part of our continuing research on the coordination chemistry of multidendentateligands**[24-27]**. We report here the preparation and characterization of schiff base ligand derived from condensation of 4amino-2, 3dimethyle-1-phenyl-3-pyrazoline-5-one with o-methyloxybenzaldehyde, p-meth-oxy benzaldehyde and 4 hydroxy-3-methoxybenzaldehyde. The study has been extended to synthesize Fe^{III}, Fe^{II}, Co^{II}, Ni^{II}, Cu^{II},

Zn^{II}, Cd^{II}, Cr^{III} complexes with the prepared ligand. All the prepared complexes have been characterized by elemental analysis, IR, HNMR, mass spectra, UV-Vis spectra, Molar Conductivity and magnetic susceptibility. Also the antimicrobial activities of all the synthesized compounds was evaluated against different antimicrobial strains. In the same direction and in continuing effect to find more potent and selective anticancer compounds, here in, anticancer activity of the prepared compounds were carried out against human tumor cell lines including colorectal cancer HCT 116.

2. Experimental

2.1. Material and Physical Measurements:

All chemical in this work were purchased from Merck without any purification. Solvent were used as received from commercial suppliers.

4-Amino antipyridine and all metal salt precursors were received from E. Merck – Elemental analysis (C, H, N, S) have been carried out in using Perkin-Elmer 2408 CHN analyser at the micro analytical center, Cairo University, Giza, Egypt. Melting or decomposition points of the prepared compounds were determined by the electrochemical melting point apparatus Goffine and Ceargemad in Britian. Metal content were determined complexometrically by standard EDTA titration**.[28]**

^{1}HNMR of L^1–L^3 and Zn(II), Cd(II) complexes were recorded on a Bruker 400 MHz Avance III HD Nanobay NMR spectrometer using DMSO–d_6 and TMS as internal standard.

IR spectra (4000-400cm^{-1}) were performed as KBr disc technique using a Perkin-Elmer 437 IR spectrometer.

The mass were recorded by Hewlett Pachard mass spectrometer model MS 5988 at the micro-analytical center, Cairo, University, Gizza, Egypt.

Magnetic susceptibilities of the metal complexes were measured by the Gouy method at room temperature using a Johnson Matthey, Alpha product, model MKI magnetic susceptibility balance. The effective magnetic moment were calculated using the relation $\mu_{eff}= 2.828\ (X_mT)^{1/2}$ B.M. where X_m is the molar susceptibility corrected using Pascal's constants for diamagnetism of all atoms in the compound.

Electronic absorption spectra of solutions of ligand and its metal complexes on DMF and the solid reflectance spectra were recorded on a Jasco model V-550 UV-Vis spectrometer.

A thermo gravimetric analyzer TGA-50 SHIMA, VZU and DTA, TA50 Shimadzu at the micro analytical center, Mubarak city for Scientific Research, Borg El-Arab, Alexandria, Egypt at the Micro analytical Center, Cairo, University, Giza, Egypt, were used to record simultaneously the IG curves, the experiments were carried out in dynamic nitrogen atmosphere (20 mL min^{-1}) with a heating rate 10°C min^{-1} in the temperature range 20-1000°C using platinum crucibles.

Molar conductance of metal complexes used highly sintered α-Al_2O_3 as a reference. The molar conductance measurements were measured in solution of the complexes in DMF (10^{-3}M) using JEN WAY 4510 conductivity meter.

2.2: Synthesis of Schiff base ligands:

The three Schiff base ligands L^1-L^3 **(Fig. 1)** were prepared by condensation of equimolar solution of 4 amino antipyrine and p-methoxybenbenzaldehyde, o-methoxybenzaldehyde and 4 hydroxy-3-methoxy benzaldehyde in absolute ethanol solution respectively. The solution was refluxed in water bath for 2 hours then cooling. After cooling, the product was filtered off, recrystallized from ethanol, washed with diethyl ether and finally dried in a desicator over anhydrous calcium chloride to give reddish brown powder of Schiff base (L^1) in 85% yield or pale orange powder of Schiff base ligand (L^2) in 70% yield and pale yellow powder of Schiff base ligand (L^3) in 87.5% yield. The proposed structure of ligands, **(Fig. 1)** is in a good agreement with the stoichiometry, calculated from their analytical data**. Table (1)**.

2.3: Synthesis of the divalent and trievalent metal complexes.

A general method has been adopted to prepare the ligand complexes in which the prepared Schiff base L^1–L^3 dissolved in ethanolicsolution. A hot ethanolic solution (50 ml) of the appropriate metal (II) chloride or sulphate and metal (III) chloride (0.01 mol) was added drop wise to a solution of ligands (L^1–L^3) (0.01 mol) with stirring. The mixture was heated under reflux for three hours on the water bath during this period, the precipitation was completed from, and collected by filtration then washed with ethanol and diethyl ether and dried in a discatorover anhydrous calcium chloride. All complexes are soluble in DMF and DMSO while insoluble in most organic solvents. These complexes were analyzed by using different available technique which agree well with the suggested molecular formula. The analytical data of the ligands and their metal complexes with their physical properties are summarized in **Table (1)**.

2.4: Antimicrobial activity:

Antimicrobial activity of all synthesized compounds, free ligands and their metal complexes were examined against various antimicrobial strains using method report in literature**[29]**. This method is the diffusion agar method **[30].** The chosen strains were *Staphylococcus aureus* (RCMB 00016), *Bacillissubtillis* (BCMB 000107) as Gram-positive bacteria, *Escherichia coli* (RCMB 000103)and *Pseudomona Aeruginosa (RCMB102)* as Gram-

negative bacteria and *Geotrichum Candidum Aspergillusfumigatu s*(RCMB002003) and *Candida Albicans* (RCMB 00502) as fungi. The antibiotic Streptomycin, Pencilling were used as standard reference in the case of Gram-positive and Gram-negative bacteria. Itraconazole and clotrinazole were used as standard antifungal reference. DMSO was used as solvent control and Sabouraud Dextrose Agar medium. The compounds were tested at concentration of 5 mg/ml against both bacterial and fungi strains.

Table (1): Analytical and some physical characteristic for the prepared L^1, L^2 and L^3 and their metal complexes (1-24)

No.	Ligand / complexes	Calcd. (found) %							Colour	Am ohm^{-1} mol^{-1} cm^2	M.wt.
		C	H	N	O	S	cl	M			
L1	L1 C19H19N3O2	71.01 69.8	5.96 5.32	13.08 12.95	9.96	-	-	-	Reddish brown	2.44	321.37
1	C19H19N3O2FeCl3(H2O)	45.50 45.01	4.22 4.13	8.38 8.28	9.57 9.37	-	21.20 21.00	11.13 11.00	Black	105.1	501.588
2	C19H19N3O2Fe(So4)2(H_2O)2	37.70 37.30	3.83 3.70	6.94 6.89	31.71 31.50	10.59 10.20	-	9.22 9.00	Reddish dark brown	86.8	608.425
3	C19H19N3O2CoCl2(H2O)2	46.84 46.30	4.76 4.66	8.62 8.52	13.13 13.00	-	14.55 14.33	12.10 12.00	Pale green	41.2	487.234
4	C19H19N3O2NiCl2(H2O)2	46.86 46.43	4.76 4.57	8.63 8.33	13.14 13.01	-	14.56 14.36	12.05 11.98	Green	20.2	487.814
5	C19H19N3O2CuCl2(H2O)2	46.40 46.20	4.71 4.69	8.54 8.33	13.01 13.00	-	14.41 14.20	12.92 12.80	Pale brown	2.19	491.854
6	C19H19N3O2ZnCl2(H2O)2	46.23 46.01	4.70 4.68	8.51 8.30	12.96 12.88	-	14.36 14.32	13.24 13.10	Pale brown	20.1	493.684
7	C19H19N3O2CdCl2(H2O)	43.66 43.20	4.05 4.00	8.04 7.99	9.18 9.01	-	13.56 13.23	21.51 21.30	Very pale yellow	133.1	540.714
8	C19H19N3O2CrCl3(H2O)	45.85 45.50	4.25 4.00	8.44 8.22	9.64 9.58	-	21.37 21.23	10.45 10.22	Pale yellow	13.13	445.738
	L2 C19H19N3O2	71.01 70.1	5.96 5.50	13.08 12.00	9.96 9.40	-	-	-	Pale yellow	98.68	321.37
9	C19H19N3O2FeCl3(H2O)	45.50 44.9	4.22 4.00	8.38 8.10	9.57 9.20	-	21.20 20.99	11.13 10.99	Dark reddish brown	101.4	501.588
10	C19H19N3O2Fe(So4)2(H2O)2	37.70 37.01	3.83 3.50	6.94 6.70	31.71 31.20	10.59 10.20	-	9.22 9.00	Pale brown	16.50	608.425
11	C19H19N3O2CoCl2(H2O)2	46.84 46.10	4.76 4.60	8.62 8.30	13.13 13.01	-	14.55 14.20	12.10 11.96	Green	33.7	487.234
12	C19H19N3O2NiCl2(H2O)2	46.86 46.50	4.76 4.60	8.63 8.30	13.14 13.01	-	14.56 14.30	12.05 12.00	Pale yellow	132.2	487.814
13	C19H19N3O2CuCl2(H2O)2	46.40 46.00	4.71 4.63	8.54 8.33	13.01 12.95	-	14.41 14.00	12.92 12.50	Dark brown	75.7	491.854
14	C19H19N3O2ZnCl2(H2O)2	46.23 45.90	4.70 4.00	8.51 8.31	12.96 12.50	-	14.36 14.10	13.24 13.00	Orange yellow	157.3	493.684
15	C19H19N3O2CdCl2(H2O)	43.66 43.01	4.05 3.89	8.04 7.92	9.18 9.00	-	13.56 13.20	21.51 21.20	Pale brown	79.7	540.714
16	C19H19N3O2CrCl3(H2O)	45.85 45.20	4.25 3.99	8.44 8.22	9.64 9.33	-	21.37 21.10	10.45 10.20	Greenish brown	43.2	445.738
	L3 C19H19N3O3	76.64 76.20	5.68 5.50	12.46 12.30	14.23 14.00	-	-	-	Pale yellow	97.4	337.372
17	C19H19N3O3FeCl3(H2O)	44.09 43.90	4.09 4.01	8.12 8.01	12.36 12.20	-	20.55 20.20	10.79 10.50	Pale brown		517.588
18	C19H19N3O3Fe(So4)2(H2O)2	36.73 36.20	3.73 3.60	6.76 6.50	33.47 33.20	10.32 10.12	-	8.99 8.80	Dark brown	19.72	624.742
19	C19H19N3O3CoCl2(H2O)2	45.35 45.10	4.61 4.50	8.35 8.10	15.90 15.50	-	14.09 14.00	11.71 11.50	Dark green	22.5	503.232
20	C19H19N3O3NiCl2(H2O)2	45.37 45.01	4.61 4.51	8.35 8.10	15.90 15.40	-	14.10 14.00	11.67 11.58	Pale brown	84.1	503.012
21	C19H19N3O3CuCl2(H2O)2	44.94 44.30	4.57 4.43	8.27 8.01	15.75 15.50	-	13.96 13.50	12.51 12.20	Greenish blue		507.852
22	C19H19N3O3ZnCl2(H2O)2	44.77 44.30	4.55 4.43	8.24 8.10	15.69 15.40	-	13.91 13.50	12.83 12.50	yellow	17.93	509.682
23	C19H19N3O3CdCl2(H2O)2	40.99 40.20	4.16 4.01	7.55 7.30	14.37 14.20	-	12.74 12.40	20.19 20.00	Yellowish white	7.47	555.712
24	C19H19N3O3CrCl3(H2O)	44.42 44.01	4.12 4.01	8.18 8.01	12.46 12.30	-	20.70 20.50	10.12 10.00	Dark brown		513.738

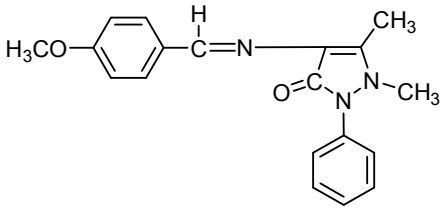

M.wt = 321.37

L^1: [4-(4-methoxy benzylidene amino)–1,5-dimethyl-2-phenyl 1,2-dihydro pyrozol-3-one.

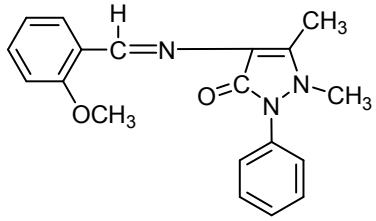

M.wt = 321.37

L^2: [4-(2-methoxy benzylidene amino)–1,5-dimethyl-2-phenyl 1,2-dihydro pyrozol-3-one.

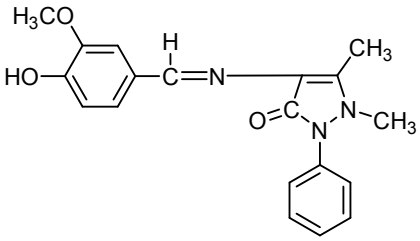

M.wt = 337.37

L^3: 4(4-hydroxy-3-methoxy benzlidene amino)-1,5-dimethy l-2-phenyl-1,2-dihydropyrazol-3-one.

Fig. 1. Structure, name and abbreviation of ligands, L^1–L^3

Method of testing

The sterilized media was poured onto the sterilized Petri dishes (20 ml, each petri dish) and allowed to solidify. Wells of 6 mm diameter were made in the solidified media with the help of sterile borer. A sterile swab was used to evenly distribute microbial suspension over the surface of solidified media and solutions of the tested samples were added to each well with the help of micropipette. The plates were incubated at 37˚C for 24 hrs in case of antibacterial activity and 48 hrs at 25°C for antifungal activity. This experiment was carried out in triplicate and Zones of inhibition were measured in mm. scale.

The antimicrobial activity were performed in the Regional for Mycology and Biotechnology, Al-Azhar University, Nasr City, Egypt.

2.5: Anticancer Activity:

2.5.1: Chemicals Used:

Dimethyl sulfoxide (DMSO), crystal violet and trypan bluedye were purchased from Sigma (St. Louis, Mo., USA).

Fetal Bovine serum, DMEM, RPMI-1640, HEPES buffer solution, L-glutamine, gentamycin and 0.25% Trypsin-EDTA were purchased from Lonza.

Crystal violet stain (1%): It composed of 0.5% (w/v) crystal violet and 50% methanol then made up to volume with ddH_2O and filtered through a Whatmann No.1 filter paper.

2.5.2: Cell lines and cultures:

Anticancer activity screening for the tested compounds utilizing human tumor colorectal cancer **HCT 116** cells (human colon cancer cell line), where obtained were obtained from VACSERA Tissue Culture Unit.

2.5.3: **Cell line Propagation:**

The cells were propagated in Dulbecco's modified Eagle's medium (DMEM) supplemented with 10% heat-inactivated fetal bovine serum, 1% L-glutamine, HEPES buffer and 50µg/ml gentamycin. All cells were maintained at 37ºC in a humidified atmosphere with 5% CO_2 and were subcultured two times a week.

2.5.4: Cytotoxicity evaluation using viability assay:

For cytotoxicity assay, the cells were seeded in 96-well plate at a cell concentration of 1×10^4 cells per well in 100µl of growth medium. Fresh medium containing different concentrations of the test sample was added after 24 h of seeding. Serial two-fold dilutions of the tested chemical compound were added to confluent cell monolayers dispensed into 96-well, flat-bottomed microtiter plates (Falcon, NJ, USA) using a multichannel pipette. The microtiter plates were incubated at 37ºC in a humidified incubator with 5% CO_2 for a period of 48 h. Three wells were used for each concentration of the test sample. Control cells were incubated without test sample and with or without DMSO. The little percentage of DMSO present in the wells (maximal 0.1%) was found not to affect the experiment. After incubation of the cells for at 37°C, various concentrations of sample were added, and the incubation was continued for 24 h and viable cells yield was determined by a colorimetric method.

In brief, after the end of the incubation period, media were aspirated and the crystal violet solution (1%) was added to each well for at least 30 minutes. The stain was removed and the plates were rinsed using tap water until all excess stain is removed. Glacial acetic acid (30%) was then added to all wells and mixed thoroughly, and then the absorbance of the plates were measured after gently shaken on Microplate reader (TECAN, Inc.), using a test wavelength of 490 nm. All results were corrected for background absorbance detected in wells without added stain. Treated samples were compared with the cell control in the absence of the tested compounds. All experiments

were carried out in triplicate. The cell cytotoxic effect of each tested compound was calculated**.** The optical density was measured with the microplate reader (SunRise, TECAN, Inc, USA) to determine the number of viable cells and the percentage of viability was calculated as [1-(ODt/ODc)]x100% where ODt is the mean optical density of wells treated with the tested sample and ODc is the mean optical density of untreated cells. The relation between surviving cells and drug concentration isplotted to get the survival curve of each tumor cell line after treatment with thespecified compound .The 50% inhibitory concentration (IC_{50}), the concentration required to cause toxic effects in 50% of intact cells, was estimated from graphic plots of the dose response curve for each conc. using Graphpad Prism software (San Diego, CA. USA)**[31].**

3-Results and Discussion

The ligands (L^1, L^2, L^3) and their metal complexes have been synthesized and characterized by spectral and analytical data. The elemental analytical data of the L^1, L^2, L^3 and their metal complexes (1-24) were in good agreement with the calculated results from the empirical formula of each compound **Table(1).** The Lower conductance values of the complexes (2.19-43 ohm^{-1} mol^{-1} cm^2) supports their non-electrolytic nature. On the other hand the molar conductivity value in the range (75-105 ohm^{-1} mol^{-1} cm^2) indicate that the complexes are 1:1 electrolytic nature **Table(1) [32,33]**.

3.1-IR Spectroscopy

The functionalities of free ligands (L^1, L^2, L^3)and their coordinating capability to form metal complexes (1-24) were invigated by IR spectroscopy. The IR spectra for the ligands and metal complexes have been recorded in the region 300-4000 cm^{-1}. The spectrum of L^1 shows absorption band at υ1589 cm^{-1} which a characteristic feature of the υ(CH=N) (azomethine) stretching mode. This band is shifted towards lower frequencies in the spectra of metal complexes in the range 1500-1508 cm^{-1} indicating the role of the azomethine nitrogen in coordination with metal ion. Also, the spectrum of L^2 shows absorption band at υ 1585 cm^{-1} which assigned to the azomethine group υ(CH=N). This band shifted to lower frequencies in the spectrum of the metal complexes ranging 1501-1562 cm^{-1} indicating the coordination takes place in azomethine nitrogen with metal ions. In addition the spectrum of L^3 gives the absorption band at υ1624 cm^{-1} assigned to the υ(CH=N) in the free ligand which shifted to lower frequencies in the spectrum of metal complexes in the range of 1512-1575 cm^{-1} indicating the coordination with metal ion **[34-37]**. The presence of the IR broad bands of free ligand L^3 and its metal complexes are in the range 3425-3521 cm^{-1} indicating to $υ_{OH}$ respectively.**[38-41]**

Table (2): The IR spectral (cm^{-1}) assignment for the ligands L^1, L^2, $L^3$and their metal complexes

No.	Ligand/complex	Chemical shift (cm^{-1})							
		υ(C=O)	υ(CH=N)	υ(N–N)	υ (M–O)	υ(M–N)	υ(–OCH_3)	υ(N–CH_3)	υ(OH)
	$L^1(C_{19}H_{19}N_3O_2)$	1643	1584	1137	--	--	2832	3047	
1	$C_{19}H_{19}N_3O_2FeCl_3(H_2O)$								
2	$C_{19}H_{19}N_3O_2Fe(SO_4)_2(H_2O)_2$	1597	1596	1099	536	443	2842	3178	
3	$C_{19}H_{19}N_3O_2CoCl_2(H_2O)_2$	1589	1589	1137	532	439	2831	2993	
4	$C_{19}H_{19}N_3O_2NiCl_2(H_2O)_2$	1597	1596	1137	532	439	2831	2993	
5	$C_{19}H_{19}N_3O_2CuCl_2(H_2O)_2$								
6	$C_{19}H_{19}N_3O_2ZnCl_2(H_2O)_2$	1593	1508	1180	532	455	2842	2985	
7	$C_{19}H_{19}N_3O_2CdCl_2(H_2O)$	1643	1589	1137	532	478	2831	2993	
8	$C_{19}H_{19}N_3O_2CrCl_3(H_2O)$								
	$L^2(C_{19}H_{19}N_3O_2)$	1643	1585	1137	--	--	2831	2935	
10	$C_{19}H_{19}N_3O_2Fe(SO_4)_2(H_2O)_2$	1500	1515	1087	621	495	2858	3190	--
11	$C_{19}H_{19}N_3O_2CoCl_2(H_2O)_2$	1609	1562	1137	678	439	2831	2935	--
12	$C_{19}H_{19}N_3O_2NiCl_2(H_2O)_2$	1601	1501	1137	624	435	2831	2935	--
13	$C_{19}H_{19}N_3O_2CuCl_2(H_2O)_2$	1635	1515	1161	694	505	2850	2920	
14	$C_{19}H_{19}N_3O_2ZnCl_2(H_2O)_2$	1593	1548	1180	682	455	2842	3039	--
15	$C_{19}H_{19}N_3O_2CdCl_2(H_2O)_2$	1608	1562	1137	671	443	2931	3128	
	$L^3(C_{19}H_{19}N_3O_3)$	1624	1581	1130	--	--	2827	2947	3425
18	$C_{19}H_{19}N_3O_3Fe(SO_4)_2(H_2O)_2$	1581	1512	1126	547	505	2839	3001	3421
19	$C_{19}H_{19}N_3O_3CoCl_2(H_2O)_2$	1585	1504	1134	555	432	2842	2947	3367
20	$C_{19}H_{19}N_3O_3NiCl_2(H_2O)_2$	1581	1508	1130	555	447	2835	3109	3350
21	$C_{19}H_{19}N_3O_3CuCl_2(H_2O)_2$	1604	1575	1126	547	424	2939	3236	3425
22	$C_{19}H_{19}N_3O_3ZnCl_2(H_2O)_2$	1585	1504	1134	555	424	2842	2943	3379
23	$C_{19}H_{19}N_3O_3CdCl_2(H_2O)_2$	1581	1512	1130	551	447	2731	2947	3521

Moreover the JR spectra showing a band at 1624-1643 cm^{-1} for the free ligands L^1, L^2 and L^3, assigned to υ(C=O) stretching mode which is shifted to lower frequency around 1581-1647 cm^{-1} indicating the coordination of the carbonyl oxygen atom of the ligand to metal ion. The coordination of the azomethine nitrogen and carbonyl oxygen was further supported by the appearance of new bands around 536-694 cm^{-1} and 424-505 cm^{-1} which are due to υ (M – O) and υ(M – N) respectively.**[35-39]**. Furthermore the other characteristic stretching absorption bands were listed in **Table(2)**.

3.2- ^{1}HNMR:

The ^{1}HNMR spectra of L^1, L^2, L^3 and their diamagnetic Zn(II), Cd(II) complexes (6, 8, 14, 15, 22, 23) have been recorded at room temperature in DMSO-d6. The ^{1}HNMR spectra of the ligands L^1, L^2 and L^3 show peaks at (*δ*)=6.80-7.76 ppm (m) endorsed to the phenyl multiplet.[**42-43]**. Schiff base L^1 also shows the following signals: C-CH3 2.42 ppm (s), N-CH3 3.11 ppm (s), oCH3 3.77 ppm(s); and azomethine proton (CH=N signal at 9.45 ppm (s). The azomethine proton (-CH=N) signal in the spectrum of Zn (II) and Cd(II) complexes are shifted at (9.50 and 9.51) ppm(s) respectively compared to the free l^1 ligand suggesting shielding of azomethine group due to the coordination with metal ion. There is no appreciate change noticed with the remaining signals of the L^1 ligand **[23,44]** and **Table(3).**

The recorded ^{1}HNMR spectra of L^2 ligand shows the following signals C-CH3 2.37 ppm(s), N-CH3 3.11 ppm(s), OCH3 3.75 ppm (s); and azomethine proton (-CH=N) signal at 9.3 ppm(s). The azomethine proton (-CH=N) signal in the spectra of Zn (II) and Cd(II) complexes are shifted downfiled at 9.45 ppm and 9.48 ppm respectively compared to the L^2 free ligand suggesting shilding of azomethine group due to complex formation. Also the other remaining signals of the complexes show no appreciable change noticed. Also ^{1}HNMR spectrum of free ligand L^3 shows the different signals at 3.78, 3.09, 2.39 ppm indicating the signals of –OCH3 (s), N-CH3 (s) and C-CH3(s) respectively. The azomethine proton (-CH=N) signal at 9.34 ppm (s) in free ligand. This signal in the spectrum of Zn(II) and cd (II) complexesare shifted downfield at 9.45 ppm and 9.44ppm respectively. In addition the ^{1}HNMR spectrum of the phenolic (OH) group in free ligand L3 and their metal complexes Zn(II), Cd(II) shows signals at 12.59 ppm which is not participate in the complexation. The ^{1}HNMR data of the ligands L^1, L^2, L^3 and their Zn(II), Cd(II) complexes are listed in **Table (3)**.

Table (3): ^{1}HNMR data of the ligands L^1, L^2, L^3 and their Zn(II), Cd(II) complexes (δ, ppm)

No.	Ligand/complex	Chemical shift (δ, in ppm)					
		CH=N azomethine	Ar–H	–OCH_3	N–CH_3	C–CH_3	OH
	$L^1(C_{19}H_{19}N_3O_2)$	9.45	6.97-7.74	3.77	3.11	2.42	
6	$C_{19}H_{19}N_3O_2ZnCl_2(H_2O)_2$	9.50	6.96-7.72	3.76	3.10	2.38	
8	$C_{19}H_{19}N_3O_2CdCl_2(H_2O)$	9.51	6.98-7.76	3.79	3.13	2.42	
	$L^2(C_{19}H_{19}N_3O_2)$	9.36	6.96-7.72	3.75	3.11	2.37	
14	$C_{19}H_{19}N_3O_2ZnCl_2(H_2O)_2$	9.45	6.98-7.72	3.78	3.13	2.42	
15	$C_{19}H_{19}N_3O_2CdCl_2(H_2O)$	9.48	7.24-7.48	3.79	3.12	2.11	
	$L^3(C_{19}H_{19}N_3O_2)$	9.34	7.30-7.49	3.78	3.09	2.39	12.59
22	$C_{19}H_{19}N_3O_2ZnCl_2(H_2O)_2$	9.45	6.80-7.50	3.79	3.09	2.39	12.5
23	$C_{19}H_{19}N_3O_2CdCl_2(H_2O)$	9.44	6.82-7.53	3.82	3.11	2.41	12.55

3.3 Electronic absorption spectrum and magnetic moment

The electronic spectra can readily provide the reliable insights about the ligand arrangement in metal complexes and also employ as a useful tool to predict geometries of the complexes. The electronic absorption spectral data for ligands and their complexes obtained in DMSO solution at room temperature at wavelength range from 200-800 nm are shown in Table (4). In the electronic spectra of the free ligands L^1, L^2 and L^3, three absorption bands were observed in the region (209, 236,339.5 nm), (252,297,343 nm) and (253,299, 563 nm) due to π-π*, n-π* and charge transferee of three ligand L^1, L^2, L^3 respectively **[45]**.

Upon complexation these transition were found to be shifted to lower or higher energy regions compared to the free ligands confirming the coordination of the ligands to the metal ion, in addition the appearance of new band at longer wavelength may be assigned to d-d transition. The magnetic moments values for Fe ^{III} complexes are 5.90-6.01 B. M. these data are closed to that reported for five unpaired electrons and confirm the octahydral geometry of these complexes. The solid reflectance of Fe^{III} complexes (1,9) displays band at 21,505 cm^{-1} for complex (1) and at 23,557 cm^{-1} for complex (9) which may be assigned to the $^6A19 \rightarrow {}^5T29(G)$ transition in octahydral geometry of these complexes.**[46]**. Also, the $^6A_{19} \rightarrow {}^5T_{19}$ transition appear as two band at (16,393-15,082 cm^{-1}) and (19,305-17,857 cm^{-1}) which

confirm the octahydral geometry of these complexes **[47]**. The diffuse reflectance spectrum of Fe (II) complexes (2, 10, 18) show two bands at (16,528-16,447 cm^{-1}) and (21,645-17,636 cm^{-1}) which are assigned to $^5T_{29} \rightarrow {}^5E_9$ transition and L-M charge transfere respectively **[48].** Also, the Fe(II) complexes showed magnetic values at the range μ_{eff} 4.6-5.01 B.M. which are consistent with an octahydral geometry **[48,49]**.

The electronic spectra of Co (II) complexes (3,11,19) of L^1- L^3 ligands display two bands at the range (15.447- 15.037 cm^{-1})and (17.857-17.047cm^{-1}) which attributed to $^4T_{19} \rightarrow {}^4T_{29}$ (F) and $^4T_{19} \rightarrow {}^4A_{29}$(F) transition respectively**[50]**.

The magnetic moment value of the Co(II) complexes is 4.7 -5.3 B.M. The spectrum resemble those reported for octahydralcomplex. The solid reflectance of the Ni (II) complexes (4, 12, 20) shows three spectral bands at (14.79-14.02 cm^{-1}), (17.76-17.42 cm^{-1}) and (25.25 -23.44cm^{-1}) which can be assigned to $^3A_{29} \rightarrow {}^3T_{29}$, $^3A_{29} \rightarrow {}^3T_{19}$(F) and $^3A_{29} \rightarrow {}^3T_{19}$ (P) transition respectively **[51]** arise due to ligand field transitions of the octahydral component of these complexes. The observed magnetic moment values μ_{eff} of 3.37, 3.14 and 3.09 B.M of L^1, L^2, L^3respectively, confirm the structure of these complexes **[51]**.

The magnetic moment values of Cu (II) complexes (5,13,21) were found to be μ_{eff} = 0.78, 0.86 and 1.002 B.M. for L^1, L^2 and L^3 respectively which confirm the octahydral structures of these complexes. These were supported by the band observed at (12, 562 cm^{-1}**,** 12.642 cm^{-1}) in the solid reflectance for complex (13.21) respectively assigned to $^2E_9 \rightarrow {}^2T_{29}$ due to octahydral structure. The band at (29,24**,** 33,670**,** 33,557 cm^{-1}) refers to L-M charge transfere**[52,53]**. The diffuse reflectance spectrum of **Cr(III)** of complexes(8, 16) of L^1, L^2 ligands display three peaks at (16,420**,** 23,310**,** 37,037 $cm^{-1)}$ for complex (8) and at (16,447**,** 20,484**,** 33,557 cm^{-1}) for complex (16) which attributed to $^4A_{29} \rightarrow {}^3T_{29}$, $^4A_{29} \rightarrow {}^3T_{19}$(F) and $^4A_{29} \rightarrow {}^3T_{19}$ (P) electronic transition respectively. The electronic transitions observed for the Cr(III) complexes suggested the octahydral geometry for the complex. The metal complexes Zn (II), Cd (II) are diamagnetic as expected for d^{10} configuration**[54]** and according to empirical formula of these complexes, we proposed an octahydral geometry for these complexes.

Table(4): The electronic spectral data of ligands L^1, L^2, L^3 and their metals complexes

No.	Ligand / complexes	π-π^*, n- π^* and charge transfer transition	d-d transition
L1	L1 $C_{19}H_{19}N_3O_2$	209, 236,339.5	-
1	$C_{19}H_{19}N_3O_2FeCl_3(H_2O)$	259, 362, 465	487, 518,610
2	$C_{19}H_{19}N_3O_2Fe(SO_4)_2(H_2O)_2$	211, 269, 462	462, 543, 605
3	$C_{19}H_{19}N_3O_2CoCl_2(H_2O)_2$	227, 270, 439	525, 605, 665
4	$C_{19}H_{19}N_3O_2NiCl_2(H_2O)_2$	218, 269, 406	521,540, 583
5	$C_{19}H_{19}N_3O_2CuCl_2(H_2O)_2$		
6	$C_{19}H_{19}N_3O_2ZnCl_2(H_2O)$	237, 267, 343	530, 602, 753
7	$C_{19}H_{19}N_3O_2CdCl_2(H_2O)_2$		558, 626,701
8	$C_{19}H_{19}N_3O_2CrCl_3(H_2O)$	209, 270, 377	429, 609
	L2 $C_{19}H_{19}N_3O_2$	252, 297, 343	-
9	$C_{19}H_{19}N_3O_2FeCl_3(H_2O)$	205, 298, 560	604,663, 677
10	$C_{19}H_{19}N_3O_2Fe(So_4)_2(H_2O)_2$	252, 297,338	567, 608, 669
11	$C_{19}H_{19}N_3O_2CoCl_2(H_2O)_2$	251,298, 328	531,617,655
12	$C_{19}H_{19}N_3O_2NiCl_2(H_2O)_2$	250, 299,569	598,659, 786
13	$C_{19}H_{19}N_3O_2CuCl_2(H_2O)_2$	251, 297, 343	532, 620, 686
14	$C_{19}H_{19}N_3O_2ZnCl_2(H_2O)_2$	217, 222,251	343, 532, 747
15	$C_{19}H_{19}N_3O_2CdCl_2(H_2O)_2$	205, 220,292	540, 620,703
16	$C_{19}H_{19}N_3O_2CrCl_3(H_2O)$	251,298, 343	541, 564, 608
	L3 $C_{19}H_{19}N_3O_3$	253, 299, 563	-
18	$C_{19}H_{19}N_3O_3Fe(So_4)_2(H_2O)_2$	208, 246, 345	608, 643, 716
19	$C_{19}H_{19}N_3O_3CoCl_2(H_2O)_2$	218, 298, 327	608, 696, 785
20	$C_{19}H_{19}N_3O_3NiCl_2(H_2O)_2$	251, 298, 346	530, 612, 715
21	$C_{19}H_{19}N_3O_3CuCl_2(H2O)_2$	251, 298, 568	598, 613, 787
22	$C_{19}H_{19}N_3O_3ZnCl_2(H_2O)_2$	218, 239, 251	346, 598, 672
23	$C_{19}H_{19}N_3O_3CdCl_2(H_2O)_2$	218, 256, 347	696, 722, 757

Table (5): Magnetic moment and electronic spectral data of L^1, L^2, L^3 metal complexes.

No.	Complex Compound	Absorption band (cm^{-1})	Band assignment	μ_{eff}(B.M)	Geometry
1	$[FeCl_3(L^1)(H_2O)]$	(16,393-19,305), 21,505	($^6A_{1g}\rightarrow{}^5T_{1g}$), $^6A_{1g}\rightarrow T_{2g}$ (G)	6.01	Octahydral
2	$[Fe(SO_4)_2(L^1)(H_2O)_2]$	16,528, 21,645	$^5T_{2g}$ (D)$\rightarrow{}^5E_g$, L$\rightarrow$MCT	5.01	Octahydral
3	$[CoCl_2(L^1)(H_2O)_2]$	15,037, 17,047	$^4T_{1g}\rightarrow{}^4T_{2g}$ (F), $^4T_{1g}\rightarrow{}^4A_{2g}$ (F)	5.12	Octahydral
4	$[NiCl_2(L^1)(H_2O)_2]$	14,025, 17,421, 25,252	$^3A_{2g}\rightarrow{}^3T_{2g}$, $^3A_{2g}\rightarrow{}^3T_{1g}$ (F), $^3A_{2g}\rightarrow{}^3T_{1g}$ (P)	3.37	Octahydral
8	$[CrCl_3(L^1)(H_2O)]$	16,420, 23,310, 37,037	$^4A_{2g}\rightarrow{}^3T_{2g}$, $^4A_{2g}\rightarrow{}^3T_{1g}$ (F), $^4A_{2g}\rightarrow{}^3T_{1g}$ (P)	-	Octahydral
9	$[FeCl_3(L^2)(H_2O)]$	15,082- 17,857), 23,557(	($^6A_{1g}\rightarrow{}^5T_{1g}$), $^6A_{1g}\rightarrow T_{2g}$ (G)	5.9	Octahydral
10	$[Fe(SO_4)_2(L^2)(H_2O)_2]$	16,447-17,636), 23,67(	$^5T_{2g}$ (D) $\rightarrow{}^5E_g$, L$\rightarrow$MCT	4.7	Octahydral
11	$[CoCl_2(L^2)(H_2O)_2]$	15,267, 17,574	$^4T_{1g}\rightarrow{}^4E_{2g}$ (F), $^4T_{1g}\rightarrow{}^4T_{2g}$ (P)	5.14	Octahydral
12	$[NiCl_2(L^2)(H_2O)_2]$	14,792, 17,574,23,444	$^3A_{2g}\rightarrow{}^3T_{2g}$, $^3A_{2g}\rightarrow{}^3T_{1g}$ (F), $^3A_{2g}\rightarrow{}^3T_{1g}$ (P)	3.14	Octahydral
13	$[CuCl_2(L^2)(H_2O)_2]$	12,562,33,670	$^2E_g\rightarrow{}^2T_{2g}$, L$\rightarrow$MCT	0.78	Octahydral
16	$[CrCl_3(L^2)(H_2O)]$	16,447, 20,484, 33,557	$^4A_{2g}\rightarrow{}^3T_{2g}$, $^4A_{2g}\rightarrow{}^3T_{1g}$ (F), $^4A_{2g}\rightarrow{}^3T_{1g}$ (P)	-	Octahydral
18	$[Fe(SO_4)_2(L^3)(H_2O)_2]$	16,447, 17,730	$^5T_{2g}$ (D) $\rightarrow{}^5E_g$, L$\rightarrow$MCT	4.6	Octahydral
19	$[CoCl_2(L^3)(H_2O)_2]$	15,447, 17,857	$^4T_{1g}\rightarrow{}^4E_{2g}$ (F), $^4T_{1g}\rightarrow{}^4T_{2g}$ (P)	5.3	Octahydral
20	$[NiCl_2(L^3)(H_2O)_2]$	14,339, 17,761, 25,239	$^3A_{2g}\rightarrow{}^3T_{2g}$, $^3A_{2g}\rightarrow{}^3T_{1g}$ (F), $^3A_{2g}\rightarrow{}^3T_g$ (P)	3.09	Octahydral
21	$[CuCl_2(L^3)(H_2O)_2]$	12,642, 33,557	$^2E_g\rightarrow{}^2T_{2g}$, L$\rightarrow$MCT	1.002	Octahydral

3.4 Mass spectra

The mass spectra of synthesized Schiff base ligands L^1, L^2 and L^3 were recorded at room temperature. The obtained molecular ion peaks confirm the proposed formulae for the synthesized compounds. The mass spectra of the L^1 Ligand depicted in **scheme (1)**.

The mass spectrum of L^1 show the molecular ion peak at m/2 321.37(11.6%) compound ($C_{19}H_{19}N_3O_2$) confirm the proposed formulae for the synthesized. Also the spectrum exhibits the strongest base peak m/z= 56 (100%) represent the stable species [$CH_2{=}CH{-}CHO$]. Moreover, the spectrum exhibits the fragment sat (m/z 76, 229, 82, 146, 119, 93, 90) corresponding to the fragment ion showed in scheme (1). The observed peaks are in good agreement with their formulae as expressed from micro analytical data **[23]**. The mass spectrum supports the proposed empirical formulae of the ligand L^2. It reveals the molecular ion peak m/z at 322 (6.01%) consistent with the molecular weight of the ligand. The mass spectrum of L^2 reveals the strongest base peak at m/z =56 (100%) represent the species [$CH_2{=}CH{-}CHO$].

The another fragments of ligand L^2 is the same of fragments of L^1 which are in good agreement with their formulae as expressed from micro analytical data **scheme (2) [23,55]**. In addition, the mass spectrum of synthesized Schiff base ligand L^3 show the molecular ion peak at m/z =337 (6.31%) which compatible with the molecular formula (C19H19N3O3). Also the mass spectrum show the base peak at m/2=56 (100%). All the remaining fragment data of ligand L^3 are shown in **scheme (3)**. Thus mass spectral data emphasize were in a good agreement with the proposed structure.

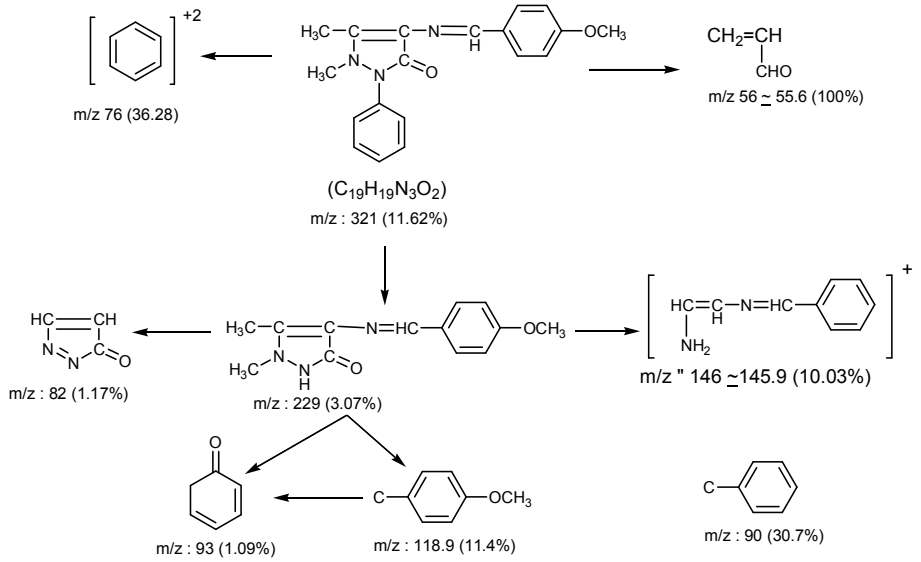

Scheme (1): Mass fragmentation pattern of L^1 ligand

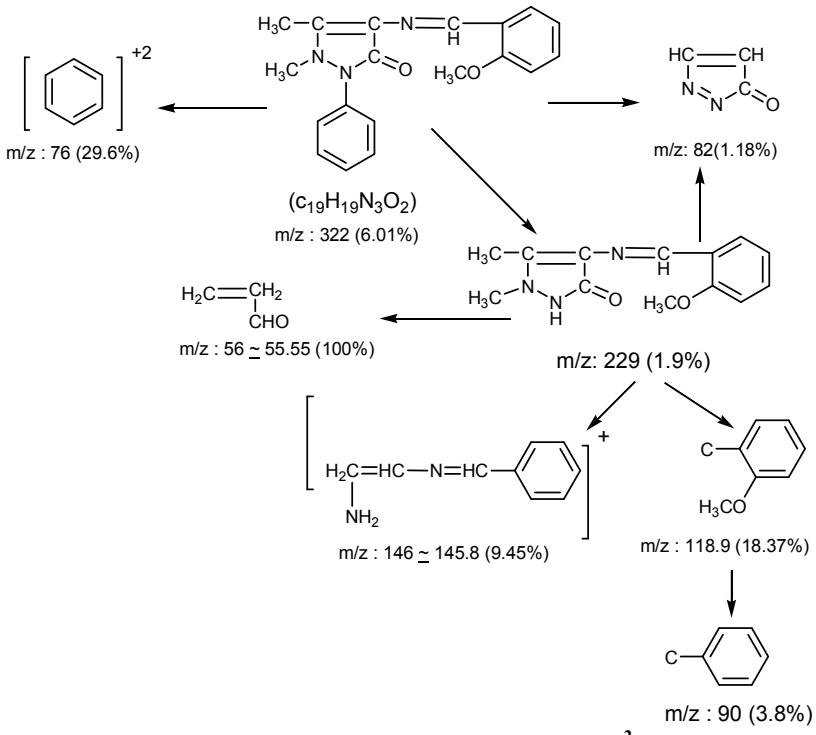

Scheme (2): Mass fragmentation pattern of L^2 ligand

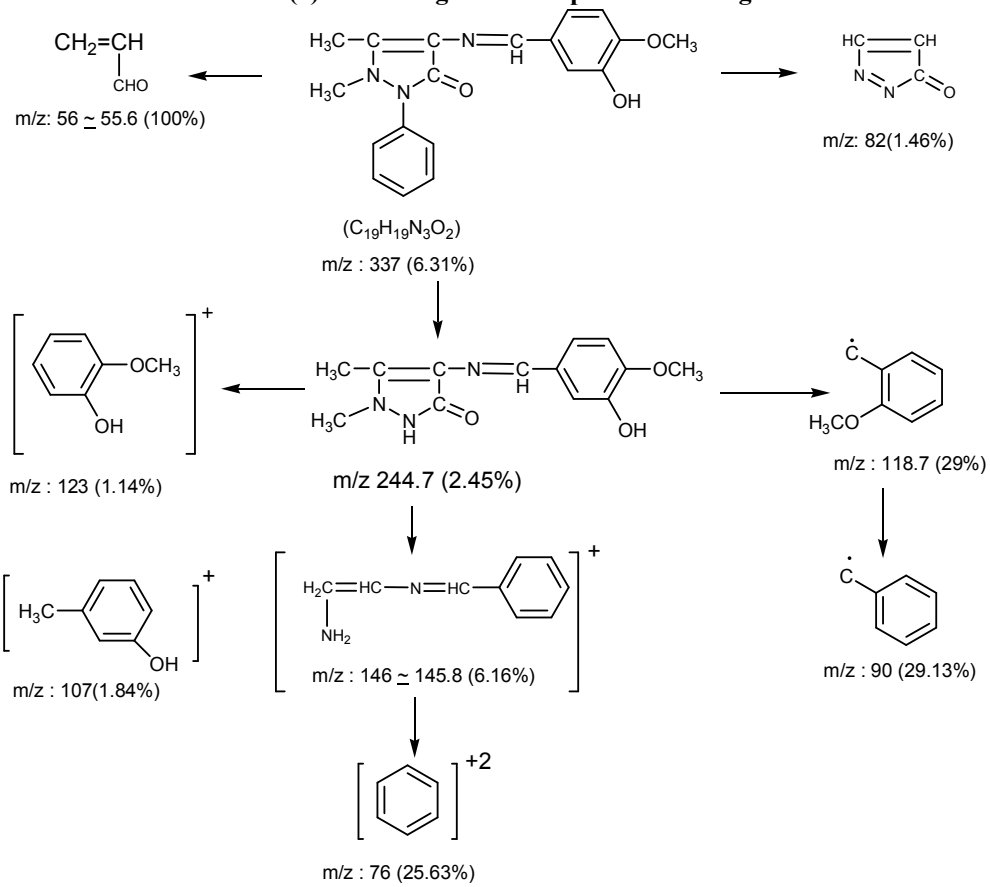

Scheme (3): Mass fragmentation pattern of L^3 ligand

3.5 Thermal Analyses (TGA and DTG):

Thermogravimetric analysis (TGA and DTA) of the metal complexes were used to get information, about the thermal stability of new complexes, decide the water molecules are inside(coordination) the inner coordination sphere of the central metal ion, and finally to suggest a general scheme for thermal decomposition of these chelates**[56].** These decomposition are measured from the ambient temperature from 30-800°c. During the heating of the metal complexes, the TG curve undergo a series of thermal changes associated with weight loss of the samples. All the thermal decomposition of metal complexes are collected in **Table (6)**.

3.6 Antimicrobial screening:

The main aim of the production and synthesis of any antimicrobial compound is to inhibit the causal microbe without any side effect on the patient **[57]**. The Schiff base complexes have provoked wide interest because they possess a diverse spectrum of biological and pharmaceutical activities. The in vitro antimicrobial activity of the ligands and their metal complexes are given in **Table (7)**. The antimicrobial activity of L^1, L^2, L^3 and their metal complexes has been tested against bacteria and fungi, since microbes can achieve the resistance to antibiotics through biochemical and morphological modification **[58]**. The antimicrobial activity of Schiff base ligands L^1, L^2, L^3 and their metal complexes were screened against micro organism, Gram positive (+ve) bacteria; *Staphylococcusaureus* (RCMB 000106) and *Bacillus stubtilis* (RCMB000107), Gram negative (-ve) bacteria pseudomonas aeruginosa (RCMB000102)and Escherichia coli (RCMB000103) and fungi *AspergillusFumigatus* (RCMB002003), Geotrichumc and idum (RCMB052006), Candida albicans (RCMB005002) and *Syncephalastrumracemosum* (RCMB00503) in order to access their potential antimicrobial agents. The antibiotic penicillin and streptomycin were used as slandered antimicrobial control and itraconazole, clotrimazole as standard fungi control using the diffusion agar technique. The action of the free ligands and their metal complexes against bacteria and fungal species with the test solution of concentration 5mg/ml were present in **Table(7)**.

The order of the activity of the metal complexes of L^1, L^2 and L^3 Schiff base ligand were shown that: Co(II) complexes for all three free ligand L^1, L^2 and L^3 were the highest values of antibacterial (gram positive bacteria, gram negative bacteria) and fungi compared with ligand, while all Fe(III) complexes were the lowest value for all antibacterial species.

Table (6): Thermogravimetric results (TG) of metal complexes of free ligands L^1, L^2L^3

No.	Complex	Temp range (°C)	n*	Loss in weight Estim. /(calcd.)% Mass loss	Total mass loss	Assignment	Metallic residue
4	$C_{19}H_{19}N_3O_2NiCl_2(H_2O)_2$	101- 190 192- 323 325- 474 476- 771	4	3.695(4.546) 23.391(23.768) 24.225(24.437) 36.234(36.198)	87.545 (88.949)	H_2O(coord.) C_8H_8N C_8H_8 $C_2H_6N_2$& 2Cl	NiO_2
6	$C_{19}H_{19}N_3O_2ZnCl_2(H_2O)_2$	289- 475 477- 907	2	31.017(31.382) 53.298(53.920)	84.315(85.741)	$2H_2O$(coord.) & C_8H_8N $C_{10}H_{11}N_3$& 2Cl	ZnO_2
1	$C_{19}H_{19}N_3O_2FeCl_3(H_2O)$	31- 204 207- 377 379- 672	3	15.384(15.061) 24.574(24.287) 37.378(37.051)	77.646(76.399)	H_2O (coord.) & C_3H_3 C_8H_2O $C_4H_6N_4$& 3Cl	FeO_2
7	$C_{19}H_{19}N_3O_2CdCl_2(H_2O)_2$	192- 486 488- 818	2	56.459(57.568) 8.914(9.705)	66.373(67.273)	$2H_2O$(coord.) & $C_7H_{13}NO_2$ H_3N_4	$CdCl_2$
13	$C_{19}H_{19}N_3O_2CuCl_2(H_2O)_2$	36- 135 104- 413 415- 726	3	3.194(3.152) 53.736(53.012) 9.211(9.469)	66.141(65.633)	H_2O coord 2Cl & $C_{16}H_{13}N_3C_3H_6$	CuO_2
15	$C_{19}H_{19}N_3O_2CdCl_2(H_2O)_2$	39- 278 280- 463 467- 796	3	7.662 (6.821) 14.900(14.548) 62.155(61.083)	84.717(84.012)	$2H_2O$ coord C_4H_4N $C_{15}H_{15}N_2$&2Cl	CdO_2
14	$C_{19}H_{19}N_3O_2ZnCl_2(H_2O)_2$	41- 250 252- 487 489- 796	3	7.290(7.103) 31.591(31.171) 47.400(47.695)	86.281(85.969)	$2H_2O$ coord C_4H_4N $C_{10}H_8N_2$ $C_9H_{11}N_2$&2Cl	ZnO_2
9	$C_{19}H_{19}N_3O_2FeCl_3(H_2O)$	24- 191 193- 323 325- 544	3	22.920(22.188) 14.662(14.355) 30.152(31.700)	67.734(68.243)	H_2O coord C_6H_4 3Cl C_9H_6	FeO_2

11	$C_{19}H_{19}N_3O_2CoCl_2(H_2O)_2$	190- 504 506- 775	2	57.457(57.303) 26.66(26.649)	84.117(83.952)	2 H_2O coord2Cl &3C1$_{11}$H$_{16}$N C_7H_5N	CoO_2
21	$C_{19}H_{19}N_3O_3CuCl_2(H_2O)_2$	41- 132 134- 329 329-550	3	5.310(4.531) 43.214(43.538) 30.417(30.584)	78.941(78.653)	$2H_2O$ coordCl& $C_{13}H_{11}NO$ $C_7H_9N_2$&Cl	CuO_2
19	$C_{19}H_{19}N_3O_3CaCl_2(H_2O)_2$	34- 459 461- 755	2	33.974(34.842) 47.881(48.376)	81.855(82.918)	$2H_2O$ coord& C_8H_9NO $C_{11}H_9N_2$&2Cl	CoO_2
23	$C_{19}H_{19}N_3O_3CdCl_2(H_2O)_2$	203- 488 490- 798	2	52.443(52.693) 21.821(21.552)	74.264(74.245)	$2H_2O$ coord & $C_{12}H_{11}NO$ $C_7H_9N_2$	CdO_2
20	$C_{19}H_{19}N_3O_3NiCl_2(H_2O)_2$	32- 132 133- 231 233-471 473- 796	4	7.155(7.226) 7.255(7.154) 26.238(25.281) 38.463(38.761)	79.111(78.422)	$2H_2O$ coord HCl C_9H_7NO $C_{10}H_{12}N_2$	NiO_2
22	$C_{19}H_{19}N_3O_3ZnCl_2(H_2O)_2$	264- 483 485- 796	2	30.992(30.841) 50.019(50.002)	81.011(80.843)	$2H_2O$ coord & $C_8H_{12}O$ $C_{11}H_9N_2$& 2Cl	ZnO_2
17	$C_{19}H_{19}N_3O_3FeCl_2(H_2O)$	27- 198 200- 380 382- 475 477- 698	4	10.594(10.536) 25.787(26.429) 14.193(14.915) 31.584(31.523)	82.158(83.403)	H_2O coord & OH 3Cl C_9H_9N $C_{10}H_{11}N_2$	FeO_2

n* = number of decomposition steps

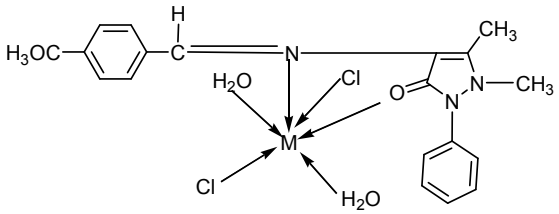

Fig. (2) Proposed structure of L^1 complexes where M = Co(II), NI(II), Cu(II), Zn(II), Cd(II), Fe(II)

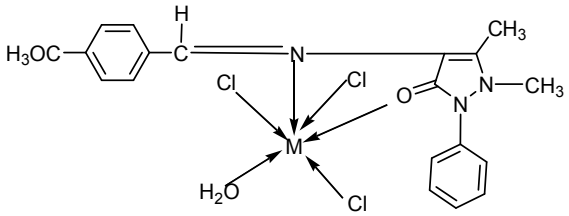

Fig. (3) Proposed structure of L^1 complexes where M = Fe(III), Cr(III)

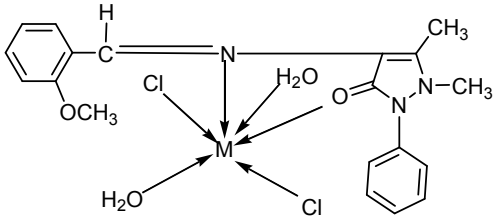

Fig. (4) Proposed structure of L^2 complexes where M = Co(II), Ni(II), Cu(II), Zn(II), Cd(II), Fe(II)

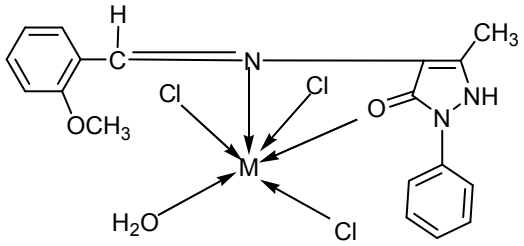

Fig. (5) Proposed structure of L^2 complexes where M = Fe(III), Cr(III)

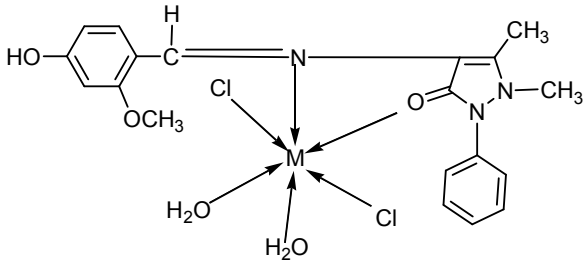

Fig. (6) Proposed structure of L^3 complexes where M = Co(II), NI(II), Cu(II), Zn(II), Cd(II), Fe(II)

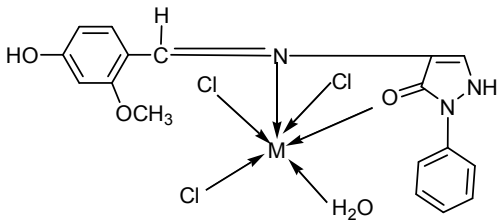

Fig. (7) Proposed structure of L^3 complexes where M = Fe(III), Cr(III)

Table (7): Antimicrobial activity of Schiff base L1, L2, L3 and their metal complexes

Test microorganism Sample	Nearest whole nm, mean of zone diameter							
Test microorganism Sample	Nearest whole nm, mean of zone diameter							
	Gram positive bacteria		Gram negative bacteria		Fungi			
	Staphylococcus aureus (RCMB 000106)	*Bacillissubtilis (RCMB 000107)*	*Preudomonas saeruginosa*(RCMB 000102)	*Escherichia coli* (RCMB 000103)	*Aspergillus funigatus* (RCMB 002003)	*Geotrichumcandidum* (RCMB 052006)	*Candida albicans* (RCMB 005002)	*Syncephalastrum racemosum* (RCMB 005003)
$L^1(C_{19}H_{19}N_3O_2)$	13.4± 0.03	14.4±0.04	NA	10.3±0.1	11.2±0.09	13.9±0.1	11.7±0.05	NA
$C_{19}H_{19}N_3O_2FeCl_3(H_2O)$	10.1±0.1	10.9±0.3	NA	7.1±0.09	11.3±0.05	9.5±0.1	8.2±0.06	NA
$C_{19}H_{19}N_3O_2Fe(SO_4)_2(H_2O)_2$	15.7±0.2	14.4±0.1	NA	13.4±0.2	13.2±0.05	14.1±0.09	12.1±0.08	NA
$C_{19}H_{19}N_3O_2CoCl_2(H_2O)_2$	19.3±0.02	20.2±0.03	16.8±0.08	18.9±0.04	18.3±0.07	20.2±0.05	17.3±0.08	13.4±0.03
$C_{19}H_{19}N_3O_2NiCl_2(H_2O)_2$	14.1±0.02	15.3±0.3	14.4±0.4	15.3±0.08	12.2±0.2	13.1±0.06	12.2±0.07	10.3±0.09
$C_{19}H_{19}N_3O_2ZnCl_2(H_2O)_2$	12.7±0.08	13.9±0.3	NA	11.8±0.6	14.2±0.09	12.5±0.3	11.4±0.2	NA
$C_{19}H_{19}N_3O_2CdCl_2(H_2O)_2$	18.9±0.3	19.5±0.1	12.2±0.2	16.7±0.09	18.6±0.01	17.2±0.08	16.5±0.2	10.1±0.09
$C_{19}H_{19}N_3O_2CrCl_3(H_2O)$	11.0±0.08	12.1±0.1	NA	12.3±0.09	12.1±0.05	11.1±0.03	10.1±0.07	NA
$L^2(C_{19}H_{19}N_3O_2)$	17.8±0.1	19.5±0.09	12.4±0.3	19.7±0.09	13.4±0.02	16.8±0.09	14.3±0.3	8.5±0.08
$C_{19}H_{19}N_3O_2FeCl_3(H_2O)$	10.8±0.05	11.4±0.3	NA	9.4±0.1	12.4±0.06	9.9±0.2	8.9±0.09	NA
$C_{19}H_{19}N_3O_2CoCl_2(H_2O)_2$	20.1±0.09	21.2±0.1	17.8±0.05	19.3±0.06	19.7±0.02	21.2±0.09	18.1±0.2	13.9±0.3
$C_{19}H_{19}N_3O_2NiCl_2(H_2O)_2$	18.9±0.3	16.3±0.2	15.8±0.4	19.9±0.04	14.5±0.5	16.8±0.05	13.9±0.04	13.5±0.09
$C_{19}H_{19}N_3O_2CuCl_2(H_2O)_2$	13.1±0.2	12.4±0.08	NA	11.1±0.2	14.5±0.03	13.5±0.09	11.7±0.08	NA
$C_{19}H_{19}N_3O_2CdCl_2(H_2O)_2$	21.3±0.09	22.2±0.3	15.7±0.08	18.3±0.05	20.4±0.09	20.1±0.07	19.4±0.08	13.5±0.02
$L^3(C_{19}H_{19}N_3O_3)$	18.6±0.1	20.2±0.2	18.6±0.3	20.4±0.4	19.7±0.09	20.2±0.07	16.8±0.05	11.4±0.05
$C_{19}H_{19}N_3O_3Fe(SO_4)_2(H_2O)_2$	17.3±0.05	16.5±0.08	NA	16.2±0.3	19.9±0.3	15.1±0.09	13.2±0.07	NA
$C_{19}H_{19}N_3O_3CoCl_2(H_2O)_2$	22.9±0.07	21.9±0.1	19.7±0.04	20.7±0.2	21.3±0.09	22.5±0.07	20.3±0.5	14.2±0.5
$C_{19}H_{19}N_3O_3NiCl_2(H_2O)_2$	20.7±0.05	21.3±0.04	18.2±0.05	21.4±0.09	18.9±0.2	20.1±0.09	17.3±0.09	15.6±0.03
$C_{19}H_{19}N_3O_3ZnCl_2(H_2O)_2$	19.2±0.09	18.7±0.2	NA	15.4±0.09	18.8±0.09	17.2±0.2	15.8±0.09	NA
$C_{19}H_{19}N_3O_3CdCl_2(H_2O)_2$	19.3±0.8	20.1±0.2	13.2±0.3	17.4±0.03	19.2±0.03	17.8±0.09	17.5±0.08	10.9±0.5

3.7: In- vitro cytotoxicity assay:

Table 8: **The *in vitro* inhibitory activity of the tested compounds against colorectal carcinoma HCT-116 cells expressed as IC_{50} values (µg/ml).**

	SampleName	IC_{50} (µg/ml)
1	L_1 ($C_{19}H_{19}N_3O_2$)	>500
2	$CoCl_2(L_1)(H_2O)_2$	422
3	$NiCl_2(L_1)(H_2O)_2$	182
4	$ZnCl_2(L_1)(H_2O)_2$	85.7
5	$CdCl_2(L_1)(H_2O)_2$	27.2
6	$Fe(So_4)_2L_1(H_2O)_2$	348
7	$CrCl_3(L_1)(H_2O)$	442
8	L_2 ($C_{19}H_{19}N_3O_2$)	>500
9	$CoCl_2(L_2)(H_2O)_2$	404
10	$NiCl_2(L_2)(H_2O)_2$	204
11	$CuCl_2(L_2)(H_2O)_2$	73.9
12	$ZnCl_2(L_2)(H_2O)_2$	243
13	$CdCl_2(L_2)(H_2O)_2$	39.1
14	$Fe(So_4)_2L_2(H_2O)_2$	>500
15	$CrCl_3(L_2)(H_2O)_2$	413
16	$FeCl_3(L_2)(H_2O)$	>500
17	$Fe(So_4)_2L_3(H_2O)_2$	298
18	L_3 ($C_{19}H_{19}N_3O_3$)	355
19	$CoCl_2(L_3)(H_2O)_2$	276
20	$NiCl_2(L_3)(H_2O)_2$	>500
21	$ZnCl_2(L_3)(H_2O)_2$	54.5
22	$CdCl_2(L_3)(H_2O)_2$	185

Evaluation of newly synthesized compound in cancer therapy were studied. In this study the antitumor activities of the synthesized compounds Schiff base ligands and their metal complexes were tested against colorectal carcinoma HCT-116 cell line. The results showed that the growth of the tested tumor cells was inhibited by all the tested compounds in dose dependent manner. Moreover, the highest inhibitory effect was reported for compound **(5)** $CdCl_2$ (27.1 µg /ml), followed by compounds 13, 21, 11, 4, 3, 22, 10, 12, 19, 17, 6, 18, 9, 15 and 2 that gives Ic_{50} values 39.1, 54.5, 73.9, 85.7, 182, 185, 204, 243, 276, 298, 348, 355, 404, 413 and 422 µg /ml, respectively against HCT-116 cells **Table (8)**.

Conclusion

Schiff base condensate ligands L^1, L^2, L^3 afford transition metal complexes which have been characterized by using elemental analysis, IR, ^{1}HNMR, UV-Vis, reflectance, magnetic susceptibility and thermal analysis. The complexes were obtained as colored powdered compounds. The elemental analysis along with metal content were in good agreement with the predicted structure. Also the reflectance spectra along with magnetic moment measurement confirm the octahydral geometry for all synthesized metal complexes. The antimicrobial activity data reveal that some complexes posses higher and other are lower activity compared to parent ligand.

This behavior in antimicrobial activity of the metal complexes may be due to the coordination with

metal ion. The results concluded that the complex containing cobalt, cadmium and nickel exhibited the highest broad-spectrum antimicrobial activities. Also the results of antitumor activities of the purified compounds confirm that the highest inhibitory effect was reported at IC_{50} value 27.1 µg /ml for compound **(5).**

References

1. K. Wajda-Hermanowicz, D. Pieniazczak, R. Wrobel, A. Zatajska, Z. Ciunik and S. Berski. 2016. Journal of Molecular Structure. 1114: 108-122.
2. N. S. Abdel-Kader, A. L. El-Ansary, T. A. El-Tayeb, and M. M. Elnagdi. 2016. Journal of Photochemistry and Photobiology A: Chemistry. 321:223-237.
3. H-Q. Chang, L. Jia, J. Xu, T-F Zhu, Z-Q. Xu, R-H Chen, etal. 2016. Mol. Struct.1106; 366-72.
4. A. Z. El-Sonbati, M. A. Diab, A. A. El-Bindary, M. I. Abou-Dobara and H. A. Seyam.2016. Journal of Molecular Liquids.218:434-456.
5. E. M. Zayed and M. A. Zayed. 2015. Spectrochimica Acta Part A: Molecular and Biomolecular Spectroscopy.143:81-90.
6. S. J. Zhang, H. Li, C. L. Gong, J. Z. Wang, Z. Y. Wu and F. Wang.2016. Synthetic Metals.217:37-42.
7. V. K. Gupta. A. K. Singh and N. Mergu.2014. Electrochimica Acta.117:405-412.
8. S. Menati, A. Azadbakht, R. Azadbakht, A. Taeb, A. Kakanajdifard. 2005. Inorg. Chem.2005; 147-57.
9. AM. Abu-Diefa, MA. Mohamed,. 2015. J. Basic Appl. Sci; 4,119-33.
10. IP. Ejidike, PA. Ajibade; 2015, Molecules 20, 9788-802.
11. R. Gannimani, A. Perumal, M. Ramesh, K. Pillay, M. E. Soliman and P. Govender, 2015. J. Mol. Struc., 1089,38.
12. M. M. Abd-Elzaher, M. M. E. Shakdof, H. A. Mous and S. A. Moustaf, SOP Trans. 2014. Appl. Chem., 1, 42.
13. A. A. Fadda and K. M. Elattar, 2015. J. Biosci. Med.,3,114.
14. S. S. Konstantinovic, B. C. Rdovanovic, Z. Cakic, V. Vasic. 2003. J serb. Chem. 68; 641-7.
15. G. Turhan-Zitouni, M. Sivaci, F. S. Kilic, K. Erol, 2001. J. Med. Chem. 36, 685-689.
16. K. Deepa, N. T. Madhu, P. K. Radhakrishnan, 2005. Met. Org. Nano-Met. Chem.33, 883-888.
17. A. A. El-Bindary, A. Z. El-Sonbati, M. A. Diab and M. K. Abd El-Kader, 2013. J. Chem., http://dx.doi.org/10.1155/2013/682186 (2013).
18. Q. H. You, P. S. Chan, W. H. Chan, S. C. K. Hau, A. W. M. Lee, N. K. Mak, T. C. W. Mak and R. N. S. Wong, 2012. RSC Adv., 2, 11078.
19. R. Shakru, Int.2015. J. Concep. Comp. Inform. Tech., 3.52.
20. M. M. Shoukry, M. R. H. Elmoghayar, M. K. A. Ibrahim and A. H. H. Elghandour, 2013. J. Chin. Chem. Soc., 34,13.
21. A. R. Ibrahim, Int. 2015. J. Adv. Res., 3, 315.
22. M. Manjunath, Ajaykumar D. Kulkarni, Gragadhar B. Bagihalli, Shridhar Malladi, Sangamesh A. Patil., 2017. J. of Molecular structure 1127, 314-321.
23. R. Paul Pandiyan, T. Arun, N. Raman, S. K. Shanuja and A. Gnanamani., 2016. International J. of Inorganic and Bioinorganic chemistry; 6 (1), 23-34.
24. MM. Abd- Elzaher; 2004a. J. Chin Chem. Soc. 51;499-504.
25. MM. Abd- Elzaher, SA. Moustafa, AA. Labib, MM. Ali. 2010; Manatsh Chem., 141;387-93.
26. MM. Abd-Elzaher, SA. Moustafa, AA. Labib, HA. Mousa, MM. Ali. 2012a. Appl. Organomet. Chem. 26; 230-6.
27. MM. Abd- Elzaher, SA. Moustafa, HA. Mousa, AA. Labib. 2012b; Moatsh Chem., 143; 909- 13.
28. G. Bassett, R. C. Denny, G. H. Geffery, J. Mendhang. Vogel' s Textbook of Quantitative (1982) Inorganic Analysis.4th ed.
29. S. A. Walksman, Microbial Antagonism and Antibiotic Substances, 72, Commonwealth Fund, N. Y., 2nd Ed 72(1947).
30. C. S. G. Kitzberger, A. S. Jr, R. C. Pedrosa, S. R. S. Ferreira (2007) J. of Food Engineering 80,631-638.
31. S. M. Gomha, S. M. Riyadh, E. A. Mahmmoud and M. M. Elaaser. (2015). Hyterocycles, 91(6):1227-1243.
32. L. M. Ying, H. P. Zhi, Z. J. Cheng, L. Yi and X. K. Xi., 2004. Chin. J. Chem. 22, 162.
33. M. Shakir, Y. Azim, H. T. N. Chishti, S. Paveen; 2006. Spectrochim Acta A 65,490.
34. Z. H. Abd El-Wahab, M. M. Mashaly and A. A. Faheim; 2005. Chem. Pap 59,25.
35. Z. Hyvaliand D. Yardimci, (2008) Trans. Met. Chem. 33,421.
36. M. Manoj kumar, K. Umasankar, S. Philipps, G. Geraldine, S. Thomas, A. Graciela, S. Robert, B. Jan, and J. Venkatesan., 2013. 67(6) 650-656.
37. A. D. Khalaji, G. Grivani, M. Rezaei, K. Fejfarova, M. Dusek. 2011. Polyhedron 30 2790-2794.
38. H. Walaa Mahmoud, G. Reem Deghadi, G. Gehad Mohamad; 2016. Appl. Organometal Chem. 30,221-230.
39. R. Rama Selvameena., 2015. J. Chem. Soc.127,4.

40. V. Gomathi, R. Selvameena, J. Rec, Sci Res. (2013) 4, 94-97.
41. K. Mounika, B. Anupama, J. Pragathi, C. Cyanakumari., 2010. J. Sci. Rec 2(3) 513-524.
42. M. A. Alaghaz, H. A. Bayoumi, Y. A. Ammar, S. A. Aldhlmani., 2013. J. Mol. Struct. 1035; 383-399.
43. A. A Abdel Aziz, A. M. Salem, M. A. Sayed, M. M. Aboaly; 2010. J. Mol. Struct.1010,130-138.
44. M. R. Maurya, S. Agarwal, C. Bader, D. Rehder., (2005). J. Inorg. chem. 2005;147-57.
45. A. A. Alhadi, Sh A. Shaker, W. A. Yehye, H. M. Ali, A. A. Mahmood, (2011) Orient. J. Chem. 27(4)1437-1442.
46. C. M. Sharapy, (2005). Spectrochimica Act A62, 326-334.
47. G. G. Mohamed., (2001) Spectrochim. Acta A 57, 1643-1648.
48. G. G. Mohamed, N. E. A. El-Gamel, F. A. Nour El-Dien (2001). Synth. React. Inorg. Met. Org. Chem 31(2) 347-358.
49. C. M. Charapy. (2005) Synth. React. Inorg. Met. Org. Chem. Part A 35, 133-142.
50. A. P. Mishra, A. Tiwari, K. J. Rajendra., (2012). Advanced Materials letters 3(3), 213-219.
51. A. S. Munde, A. N. Jagdale, S. M. Jadhav et al., (2010). J Serb. Chem. Soc. 75(3),349-359.
52. M. S. Suresh and V. Prakash., (2010) Inter. J. of the Physical Science 5(14):2203-2211.
53. S. chandra, R. K. Qanugo, S. K. Sharma, Spectrochim. 2012 Spectrochim. Acta A, 94,312-317.
54. S. Chandra, L. K. Gupta. (2005). Spectrochim, Acta A 61, 1181.
55. M. M Abd-Elzaher, A. A Labib, H. A. Mousa, S. A. Moustafa, M. M. Ali, A. A. El-Rashady. (2016). Beni-Suef University Journal of Basic And Applied Sciences. (5) 85-96.
56. G. G. Mahamed, M. M. Omar, A. M. Hindy. (2006) Turk J. Chem.30,361-382.
57. M. M. H. Khalil, E. H. Ismail, G. G. Mohamed, E. M. Zayed, A. Bader. (2012) J. Inorg. Chem. 2,13-21.
58. G. G Mohamed. (2006). Spectro-Chim. Acta Part A 64,188-195.

3/7/2017